Internal vibrations of a vector soliton in the coupled nonlinear Schrödinger equations

Boris A. Malomed*
Department of Interdisciplinary Studies, Faculty of Engineering, Tel Aviv University, Tel Aviv 69978, Israel

Richard S. Tasgal†
Department of Applied Mathematics, School of Mathematical Sciences, Tel Aviv University, Tel Aviv 69978, Israel

(Received 8 October 1997; revised manuscript received 21 April 1998)

Static and dynamic properties of a two-component soliton are studied via the variational approximation (VA), consideration of the radiation spectrum, and direct numerical simulations. The VA, based on a Gaussian *Ansatz*, proves to be (as compared to the direct simulations) fairly accurate in some respects and inaccurate in others—in particular, the predictions for the widths of the stationary states are about a sixth part greater than the actual widths. We formulate an empirically modified version of the variational approximation: at the end of the analysis, the Gaussian is replaced by sech with properly rescaled widths. This hybrid VA yields extremely accurate predictions for the stationary states. The error in the width prediction is $\lesssim 1\%$, and simulations demonstrate minuscule radiation losses. The VA model predicts three eigenmodes of the soliton's internal vibrations, all of which are observed numerically. Oscillation of the separation between the two components is found to be the most persistent mode, and in-phase oscillation of the two widths is the next most persistent one; in contrast, the out-of-phase width oscillations are unstable, quickly rearranging themselves into the stable in-phase mode. These features are easily explained by comparing the corresponding vibrational eigenfrequencies to the spectral gaps which isolate oscillations localized at the soliton from delocalized radiation modes. For vector solitons with energy nearly equally divided between the components, the analysis reveals a remarkable feature: *saturation* of the separation oscillations, with the radiative decay virtually ceasing at a finite level of the mode's amplitude. The relatively stable in-phase width-oscillation mode decays indefinitely, but according to a very slow power law rather than exponentially. Lastly, for large-amplitude vibrations, the VA models predict dynamical chaos, but, due to the quick decay of the large oscillations, direct simulations show no chaos. [S1063-651X(98)05408-7]

PACS number(s): 42.81.Dp, 42.65.Re, 03.40.Kf

I. INTRODUCTION

Despite great progress in characterizing solitons in a wide variety of situations, one of the most fundamental cases, vector solitons governed by a pair of coupled nonlinear Schrödinger (NLS) equations, defies solution in some important respects. The coupled NLS model and its vector soliton solutions have a number of interesting physical applications, the most important of which is a bimodal optical fiber, where the coupled NLS equations govern light propagation in the two polarization components [1]. Except for the special case of the Manakov system [2], with equal self-phase and cross-phase modulation coefficients (which is not the case in the real bimodal fiber), when the coupled NLS equations are integrable, exact analytical results, such as expressions for stationary solitons with arbitrary polarization, or a rigorous knowledge of how quickly internal vibrations of a perturbed vector soliton fade through emission of radiation, are absent (though, an important contribution to the latter issue was recently made by Yang [3]).

The coupled NLS equations can be well simulated by contemporary numerical techniques. Nevertheless, in the absence of nontrivial exact solutions, approximate analytic methods remain (in conjunction with direct simulations) quite useful. In this work, we employ the variational approximation (VA) based on the averaged Lagrangian [4], supplemented by direct consideration of eigenfrequencies of the vector soliton's internal modes with respect to the spectrum of the linearized equations (which will turn out to complement the VA in a very helpful way). The VA approximates a soliton by an *Ansatz* having a few free parameters, with the soliton's known qualitative features built in, and flexible enough to accommodate as yet unknown features. The *Ansatz* is substituted into the Lagrangian density of the governing partial differential equations (PDEs), which is then explicitly integrated over the temporal variable, leaving a dependence only on the propagation distance (which is the evolutional variable for the optical fibers or waveguides [1]). The Euler-Lagrange equations following from this averaged Lagrangian are a set of ordinary differential equations (ODEs) for the *Ansatz*'s parameters, approximating the system's dynamics.

In the integrable limits of the coupled NLS equations, the vector solitons take a hyperbolic secant (sech) shape [2,5]. Although this does not hold true for the general (nonintegrable) case, it is not unreasonable to expect sech profiles to be good approximations. For example, the variational method with the sech approximation was used to model vector solitons in a pair of coupled NLS equations in Refs. [6] and [7]. The disadvantage of this is that, in order to make the integrals in the VA analytically soluble, the pulse widths in the two polarization components must be postulated to be identical, whereas, in reality, the pulse widths of the two

*Electronic address: malomed@eng.tau.ac.il
†Electronic address: tasgal@math.tau.ac.il

components are often far from equal. In the physically most important case of the linear ellipticity, for example, the widths may differ by one-sixth [8]. A well-known alternative is a Gaussian *Ansatz* [4]. This is in some respects a less accurate approximation for the soliton shape, but can accommodate important features (such as the unequal widths), that the sech *Ansatz* cannot [4,8–11].

In this work, we formulate an empirically improved version of the VA, combining elements of both the Gaussian and sech-based models. The calculations are based on a Gaussian *Ansatz*, with an *ad hoc* modification of the results to the sech shape *at the end* of the analysis. We compare the predictions of the usual Gaussian-based VA and of the newly proposed hybrid model with direct numerical simulation of the PDEs, focusing especially on the predictions which the Gaussian VA makes but which the sech model cannot.

The results show that the usual Gaussian VA is generally accurate, save for the numerically observed relaxation of the vector solitons from their predicted Gaussian shapes to the final sechlike ones. This proviso is not insignificant, as, in the course of the relaxation, the pulse's full width at half maximum (FWHM) drops by about one-sixth before reaching equilibrium, and this readjustment process occludes other more subtle effects. In contrast, our hybrid (but essentially Gaussian) VA yields excellent predictions for the static solutions, especially for the vector soliton's widths, which are at worst only about 1% greater than the exact numerical result, and are usually much better than that. Another strength of the hybrid VA is related to the radiative losses: while the configurations produced by the usual Gaussian approximation lead, in direct simulations, to about 99% of the energy trapped into the vector soliton and 1% being lost to dispersive radiation, the hybrid VA ends up with virtually all the energy remaining in the soliton (numerical simulations showed no detectable emitted radiation). The latter feature is a significant asset of this version of the VA, since variational methods cannot easily accommodate and therefore typically omit the radiation component of the solution (see Ref. [11] for a rare exception). Thus an *Ansatz* which, on comparison with numerical simulation, gives rise to (virtually) no emission of radiation has a crucial advantage.

The second objective of this work is an accurate quantitative analysis of internal vibrations of the vector soliton by means of both the VA and direct simulations. This problem is important for solitons in optical fibers, especially narrow solitons with widths of few picoseconds or less, for which the soliton period is short enough ($\sim$1 km) to allow direct experimental observation of the soliton's internal dynamics. The VA predicts three small vibrational eigenmodes [8] about the soliton's steady state. Direct PDE simulations demonstrate that the most persistent of the predicted modes is oscillation of the separation between the centers of the two polarization components. After that, the next most persistent mode is the one in which the widths of the two components oscillate in phase. The third mode, out-of-phase width oscillations, turns out to be conspicuously unstable. The instability, however, is not with respect to the emission of radiation, but rather with respect to the in-phase width oscillations: a vector soliton initially vibrating out of phase tends to quickly rearrange itself into the one with stable in-phase width oscillations. We can explain the robustness of the separation-oscillation and in-phase width-oscillation modes, as well as the instability of the out-of-phase one, by comparing the eigenfrequencies of these modes with the gaps that insulate the small oscillation modes localized at the soliton from the continuum spectrum of the delocalized radiation modes. We find that the most robust oscillation mode (the separation between the centers) is located inside the gap; the second most robust mode (the in-phase width oscillations) is almost exactly at the gap's edge; and the unstable mode (the out-of-phase width oscillations) lies outside the gap, well inside the continuum spectrum. This means that the out-of-phase width oscillation is not a true eigenmode of the full linearized problem, but rather a so-called quasimode (cf. a known quasimode of the two-component optical soliton in the second-harmonic-generating medium [12]).

When the energy of the steady state is evenly divided between the polarization components, the predictions for the in-phase vibrational mode given by the VA prove (on comparison with direct simulation) to be fairly good. But in the case of a more general polarization, when one component has more energy than the other, the more energetic component tends to oscillate as if by itself, with the less-energetic one following along but not (contrary to the VA predictions) contributing in an equal fashion to the oscillations.

An issue of special interest is the possibility of chaotic internal vibrations of the soliton (see, for example, the recent work [13] where this issue was considered in the framework of the Zakharov model). We find that the ODE description produced by the VA does exhibit dynamical chaos, provided that the amplitude of the vibrations is large enough (but still under the threshold for escape or complete radiative decay, i.e., splitting of the vector soliton into two single-component solitons, or unlimited growth of the widths [8]). However, direct PDE simulations demonstrate that the above-mentioned instability quickly switches off the out-of-phase mode, and the loss of this degree of freedom, together with (nonradiative) damping of large-amplitude oscillations in the other modes, causes the degeneration of would-be chaotic oscillations into regular ones.

Yang [3] very recently studied the vibrations of and emission of radiation from the vector solitons via a different method. Based on a straightforward linearization of the equations about the static solution, Yang found exact small vibrational solutions in a few special cases, and elaborated algorithms for determining the true form of the small vibrations numerically in the general case. Reference [3] represents a great advance in understanding the dynamics of small vibrations of the vector solitons. The very sophistication of the methodology, however, makes the general results cumbersome to obtain and work with, and obscures some important results under a mass of analytic and numerical apparatus. Our methodology provides a well-motivated and heuristic description of the essential phenomena, leading to fairly accurate predictions, as compared to the direct simulations. The flexibility and relative technical simplicity of the combined technique developed in the present work greatly assists analysis of the numerical observations; thus we confirm some of the results of Ref. [3] for *small* oscillations, finding disagreements in some other cases, and we obtain interesting results for *nonsmall* oscillations, which are for the most part beyond the scope of Ref. [3]. In particular, we conclude that

the amplitude of the relatively stable in-phase width-oscillation mode decays indefinitely according to a power law, while the decay of the most stable separation mode *saturates*, leaving a virtually constant finite residual value of its amplitude. The latter result, predicting finite-amplitude persistent relative oscillations of the two components of the vector soliton, has clearly important physical consequences for optical fibers. It should be easy to observe experimentally by means of polarization filters and the usual autocorrelation technique [1] in a bimodal optical fiber. Taking a moderately narrow soliton with temporal width of few picoseconds, a fiber length of several kilometers will be sufficient. The initial perturbation exciting the separation mode can be generated by a short additional fiber segment with a strong group-velocity birefringence.

II. GAUSSIAN APPROXIMATIONS—USUAL AND HYBRID

A. Basic equations

The basic governing equations for the light propagation in a bimodal nonlinear optical fiber are the well-known coupled NLS equations [1]

$$iu_z+\tfrac{1}{2}u_{tt}+(|u|^2+B|v|^2)u=0, \tag{1a}$$

$$iv_z+\tfrac{1}{2}v_{tt}+(B|u|^2+|v|^2)v=0. \tag{1b}$$

The variables $u(z,t)$ and $v(z,t)$ are the amplitudes of the electromagnetic waves in each of the polarization modes, z is the propagation distance, and t is the reduced time (in the reference frame moving along with the carrier wave). Equations (1) omit some terms which are in the present context inconsequential—the phase-velocity and group-velocity birefringence, and four-wave mixing. These terms are omitted not because they are small, but rather because (except for some special cases—see, for example, Ref. [14]) they either can be eliminated by simple transformations, or have nearly zero net effect due to self-averaging.

In this work, all the numerical simulations are done for the linear birefringence case—the most important one for the optical fibers—which has the nonlinear cross-coupling coefficient in Eqs. (1) $B=\frac{2}{3}$ [1]. The analytic part of the study, however, will be kept general, valid for any positive value of B.

As an approximation for the vector soliton generated by the coupled NLS equations (1), we choose the Gaussian *Ansatz*

$$u(z,t)=A_u\exp\left[-\frac{1}{2}\left(\frac{t-y_u}{W_u}\right)^2\right]\exp[i(a_u+b_u(t-y_u)+c_u(t-y_u)^2)], \tag{2a}$$

$$v(z,t)=A_v\exp\left[-\frac{1}{2}\left(\frac{t-y_v}{W_v}\right)^2\right]\exp[i(a_v+b_v(t-y_v)+c_v(t-y_v)^2)], \tag{2b}$$

where all the parameters are functions of the propagation distance z. *Ansatz* (2) accommodates a pulse with arbitrary amplitudes (A_u,A_v), widths (W_u,W_v), and central positions (y_u,y_v). Each component can also have any phase (a_u,a_v), central frequency (b_u,b_v), and frequency chirp (c_u,c_v). Not allowed by the *Ansatz* are the emission of dispersive radiation or more complicated changes in the vector soliton's shape. Notice, however, that the *Ansatz* does admit splitting of the vector soliton into single-component ones [8].

The averaged Lagrangian variational method, with *Ansatz* (2) and governing equations (1), yields a set of equations for all the twelve parameters of the *Ansatz* [8]. They include four integrals of motion and six nontrivial evolutional equations (which we write below as three second-order equations). There are also equations for two variables, the phases a_u and a_v, which involve other variables but do not themselves influence anything else, so are not displayed below. The integrals of motion are the energies $E_{u,v}$ in the components

$$E_u\equiv\int_{-\infty}^{\infty}|u|^2dt=\sqrt{\pi}A_u^2W_u, \tag{3a}$$

$$E_v\equiv\int_{-\infty}^{\infty}|v|^2dt=\sqrt{\pi}A_v^2W_v, \tag{3b}$$

the total momentum P,

$$P\equiv\int_{-\infty}^{\infty}\frac{i}{2}(u_tu^*-uu_t^*+v_tv^*-vv_t^*)dt=\frac{d}{dz}(E_uy_u+E_vy_v)\equiv-(E_ub_u+E_vb_v), \tag{3c}$$

and the Hamiltonian of Eqs. (1), which we will not need in an explicit form. It is convenient to define the soliton's polarization angle θ [8] by $\tan^2\theta\equiv E_v/E_u$, which allows us to write $E_u=(E_u+E_v)\cos^2\theta$ and $E_v=(E_u+E_v)\sin^2\theta$. If the widths were equal—which is not generally the case—then the amplitudes of the components u and v would be proportional, respectively, to $\cos\theta$ and $\sin\theta$.

The remaining nontrivial equations of motion for the widths $W_{u,v}$ and relative position $y\equiv y_u-y_v$ of the vector soliton's components are

$$\frac{d^2}{dz^2}W_u=W_u^{-3}-\frac{E_u}{\sqrt{2\pi}}W_u^{-2}-\frac{2B}{\sqrt{\pi}}E_vW_u(W_u^2+W_v^2)^{-3/2}\times\left(1-\frac{2y^2}{W_u^2+W_v^2}\right)\exp\left(-\frac{y^2}{W_u^2+W_v^2}\right), \tag{4a}$$

$$\frac{d^2}{dz^2}W_v=W_v^{-3}-\frac{E_v}{\sqrt{2\pi}}W_v^{-2}-\frac{2B}{\sqrt{\pi}}E_uW_v(W_u^2+W_v^2)^{-3/2}\times\left(1-\frac{2y^2}{W_u^2+W_v^2}\right)\exp\left(-\frac{y^2}{W_u^2+W_v^2}\right), \tag{4b}$$

$$\frac{d^2}{dz^2}y=\frac{d}{dz}(-b_u+b_v)=-\frac{2B}{\sqrt{\pi}}(E_u+E_v)(W_u^2+W_v^2)^{-3/2}y\times\exp\left(-\frac{y^2}{W_u^2+W_v^2}\right), \tag{4c}$$

while the chirp parameters c_u and c_v are expressed in terms of the widths as follows: $c_u=(2W_u)^{-1}(d/dz)W_u$ and $c_v=(2W_v)^{-1}(d/dz)W_v$.

B. Fixed points

The fixed points of Eqs. (4) correspond to steady-state vector solitons, with the stationary values $y=c_u=c_v=0$ and [8]

$$W_u=\frac{\sqrt{2\pi}}{E_u}\left[1-Br^4\left(\frac{2}{r^2+1}\right)^{3/2}\right]\Big/\left[1-B^2\left(\frac{2r}{r^2+1}\right)^3\right], \tag{5a}$$

$$W_v=\frac{\sqrt{2\pi}}{E_v}\left[1-Br^{-1}\left(\frac{2}{r^2+1}\right)^{3/2}\right]\Big/\left[1-B^2\left(\frac{2r}{r^2+1}\right)^3\right], \tag{5b}$$

where the width ratio $r\equiv W_u/W_v$ is determined by the equation

$$B\left(\frac{2}{1+r^2}\right)^{3/2}\left(r^4-\frac{E_v}{E_u}\right)+\frac{E_v}{E_u}r-1=0. \tag{5c}$$

Thus, the energies of the two components E_u and E_v are free parameters of the stationary vector soliton, the amplitudes A_u and A_v being determined by the energies and the widths (5) according to the relationships (3a) and (3b).

While the relative frequency (b_u-b_v) is zero at the fixed point, the mean frequency $(b_u+b_v)/2$ can take any constant value, a nonzero one adding a net momentum to the soliton. The phases a_u and a_v vary linearly with z at the fixed points, which, however, does not affect the other parameters of the *Ansatz*. Finally, all this is inserted back into *Ansatz* (2) to produce a (predicted) vector soliton wave form.

Table I summarizes the predictions produced by the VA for the parameters of the stationary vector soliton for the physically most important value $B=\frac{2}{3}$ and a range of polarization angles. The Hamiltonians in the table are of the usual Gaussian model (2), while the values of the widths refer to either the Gaussian *Ansatz* [Eqs. (2)] with total energy $E\equiv E_u+E_v=\sqrt{2\pi}$, or (see below for a description) the hybrid Gaussian-sech *Ansatz* [Eqs. (6b) and (6c)] with $E=2$. Note that the negativeness of the Hamiltonian is a necessary stability condition for the soliton (if the Hamiltonian were positive, the soliton would decay into radiation). The stationary widths for other values of the energies can be obtained from Table I: in either *Ansatz*, the widths scale as the reciprocal of the total energy E, so, to obtain the widths for arbitrary total energy E, the values borrowed from Table I should be multiplied by $(\sqrt{2\pi}/E)$ or $(2/E)$, for the Gaussian or sech approximations, respectively. For polarization angles greater than 45°, one should take the complement of the angle and interchange u and v.

TABLE I. The widths of the two components predicted for the stationary vector soliton by the variational approximation, based on the Gaussian *Ansatz* with total energy $E=\sqrt{2\pi}$, or the sech *Ansatz* with total energy $E=2$, for a range of values of the vector soliton's polarization angle θ. The values of the vector soliton's Hamiltonian refer to the Gaussian *Ansatz*. The cross-coupling coefficient is $B=\frac{2}{3}$.

Polarization	Hamiltonian	W_u	W_v
$\theta=0°$	−0.500	1.0000	n/a
$\theta=5°$	−0.495	1.0038	1.1881
$\theta=10°$	−0.481	1.0149	1.1930
$\theta=15°$	−0.460	1.0330	1.2003
$\theta=20°$	−0.435	1.0571	1.2089
$\theta=25°$	−0.408	1.0860	1.2168
$\theta=30°$	−0.384	1.1175	1.2220
$\theta=35°$	−0.364	1.1489	1.2220
$\theta=40°$	−0.352	1.1774	1.2150
$\theta=45°$	−0.347	1.2000	1.2000

C. Modification of the Gaussian approximation

In the exactly solvable cases, the vector solitons predicted by the Gaussian *Ansatz*'s fixed points differ from the exact shapes in a simple way which suggests a transformation to improve the predictions of the Gaussian-based VA in the general case. The available exact solutions [in the cases $B=0$, $B=1$, or arbitrary B with $u(z,t)=v(z,t)$] for the soliton with given energy take a sech form [2,5], $|u|=A^{\rm sech}\,{\rm sech}(t/W^{\rm sech})$, with the width and amplitude related to those of the Gaussian *Ansatz* (2), in all the cases, as follows:

$$W^{\rm sech}=\sqrt{2/\pi}W^{\rm Gauss},\quad A^{\rm sech}=\sqrt{\pi/2^{3/2}}A^{\rm Gauss}. \tag{6a}$$

Note that these relations have the sech *Ansatz*'s energy, $E=2(A^{\rm sech})^2W^{\rm sech}$, equal to the Gaussian *Ansatz*'s energy. The other parameters, except for the (unimportant) phases, are the same as in the Gaussian approximation.

This suggests that making the same adjustment in the *final* results produced by the Gaussian-based VA—replacing the Gaussian by a sech pulse with the parameters rescaled according to Eqs. (6a)—may in effect cancel some of the distortions caused by the *Ansatz*'s artificially forcing the pulse to take a Gaussian shape, even in the cases when exact solutions are not available.

To estimate the importance of the adjustment, we note that if, in the soluble cases, all the energy of the Gaussian initial pulse were to go into the final sech pulse, its (standardly defined) FWHM width would end up a factor $[(\sqrt{2}\,\cosh^{-1}\sqrt{2})/\sqrt{\pi\,\ln 2}]\approx 0.845$ smaller than at the start.

For the exact soliton, this adjustment yields the exact solution; therefore this adjustment *exactly* cancels *all* the distortions. There is no reason in the general case for the can-

TABLE II. The modal eigenvectors and the corresponding eigenfrequencies for the small internal vibrations of the vector soliton, as predicted by the variational approximation based on the Gaussian *Ansatz* with total energy $E=\sqrt{2\pi}$, at different values of the polarization angle θ.

Polarization	Separation	In-phase mode	Out-of-phase mode
$\theta=0°$	$k(1,0,0)=$ n/a	$k(0,1,1)=1$	$k(0,1,-1)=$ n/a
$\theta=5°$	$k(1,0,0)=0.7079$	$k(0,\ 1,\ 4.66)=0.9826$	$k(0,\ 1,\ -28.3)=1.0720$
$\theta=10°$	$k(1,0,0)=0.7005$	$k(0,\ 1,\ 3.50)=0.9443$	$k(0,\ 1,\ -9.20)=1.0816$
$\theta=15°$	$k(1,0,0)=0.6891$	$k(0,\ 1,\ 2.71)=0.8973$	$k(0,\ 1,\ -5.13)=1.0841$
$\theta=20°$	$k(1,0,0)=0.6748$	$k(0,\ 1,\ 2.19)=0.8473$	$k(0,\ 1,\ -3.44)=1.0790$
$\theta=25°$	$k(1,0,0)=0.6593$	$k(0,\ 1,\ 1.82)=0.7989$	$k(0,\ 1,\ -2.53)=1.0683$
$\theta=30°$	$k(1,0,0)=0.6492$	$k(0,\ 1,\ 1.54)=0.7562$	$k(0,\ 1,\ -1.95)=1.0549$
$\theta=35°$	$k(1,0,0)=0.6321$	$k(0,\ 1,\ 1.32)=0.7230$	$k(0,\ 1,\ -1.54)=1.0424$
$\theta=40°$	$k(1,0,0)=0.6240$	$k(0,\ 1,\ 1.15)=0.7017$	$k(0,\ 1,\ -1.24)=1.0333$
$\theta=45°$	$k(1,0,0)=0.6211$	$k(0,1,1)=0.6945$	$k(0,1,-1)=1.0300$

cellation of the distortion to be this good. If fact, these are the only cases when it is perfect; in the general case, this adjustment can only be expected to cancel out the main distortion. It will be shown below that for static solutions, the result is extremely good. For dynamic solutions, as will be shown below, agreement with the full numerical simulation ranges from very good to merely reasonable. This disagreement may not be due to the Gaussian *Ansatz per se*, but rather to the fact of the variational approximation.

The most critical difference between the Gaussian and sech wave forms is that the Gaussian's tails have much less energy than the sech's exponential tails, or, expressed differently, the Gaussian is more compact than the hyperbolic secant. This difference is most important when the components of the soliton are widely separated, in which case the Gaussian greatly underestimates the Hamiltonian for the coupling between the two components. This regime is not the focus of the present work. Accurate representation of the tail is much more important for ''light bullets'' in the multidimensional case (bulk media) than it is for one-dimensional solitons in optical fibers [19].

In more explicit mathematical form, we take a solution to Eqs. (4), which govern the evolution of the Gaussian *Ansatz*'s parameters, but insert the parameters not into the Gaussian ansatz (2) but rather into

$$u(z,t)=A_u^{\mathrm{sech}}\ \mathrm{sech}\left(\frac{t-y_u}{W_u^{\mathrm{sech}}}\right)\exp[i(a_u+b_u(t-y_u)+c_u(t-y_u)^2)], \tag{6b}$$

$$v(z,t)=A_v^{\mathrm{sech}}\ \mathrm{sech}\left(\frac{t-y_v}{W_v^{\mathrm{sech}}}\right)\exp[i(a_v+b_v(t-y_v)+c_v(t-y_v)^2)], \tag{6c}$$

with the widths and amplitudes rescaled according to Eq. (6a). Despite the *ad hoc* nature of this adjustment, the heuristic motivation given above makes it promising. In Sec. II D, we check the results against direct numerical simulation of the underlying PDE's (1), and conclude that our approach indeed provides for a drastic improvement of the accuracy.

D. Vibrations

Large vibrations and other dynamics can only be completely understood via the full set of the dynamical equations (3) and (4). For small vibrations, eigenmodes of the linearized ODE's can be found using standard methods [8]. There is no need to display all the involved but straightforward details here. The essential results are that small vibrations of the separation y decouple from those of the widths W_u and W_v. Two distinct eigenmodes of the width vibrations can be identified, one ''in phase,'' with both widths decreasing and increasing synchronously, and the other one ''out of phase,'' with the two widths oscillating with a phase shift π. At polarization angles $\theta=0°$ to $\theta=45°$, with the total energy $E=\sqrt{2\pi}$, the modal eigenvectors (the components of which are the deviations of y, W_u, and W_v from their steady-state values) and their associated frequencies are collected in Table II (the ''frequencies'' are here *spatial* frequencies, or propagation constants, because the evolutional variable is the propagation distance z). To obtain the eigenmodes for the total energy different from $\sqrt{2\pi}$, one should scale the frequencies in proportion to the energy squared. For polarization angles θ between 45° and 90°, it is sufficient to take the complement of the angle, $(90°-\theta)$, and interchange u and v.

The particular case $\theta=0°$ corresponds to the single-*(u)* component soliton. With zero energy in v, only one of the vibrational modes can exist. The case $\theta=45°$ is the soliton with the energy split half-and-half between the components u and v. The analytic solutions for the eigenvectors and the associated eigenfrequencies (propagation constants) of the $\theta=45°$ Gaussian pulses with an arbitrary cross-phase modulation coefficient B are

$$k^{\mathrm{Gauss}}(1,0,0)=B^{1/2}\left(\frac{1+B}{2}\right)^{3/2}\frac{E^2}{2\pi}, \tag{7a}$$

$$k^{\mathrm{Gauss}}(0,1,1)=\left(\frac{1+B}{2}\right)^{2}\frac{E^2}{2\pi}, \tag{7b}$$

$$k^{\mathrm{Gauss}}(0,1,-1)=\sqrt{1+\frac{3B}{1+B}}\left(\frac{1+B}{2}\right)^{2}\frac{E^2}{2\pi}. \tag{7c}$$

It is useful to compare these expressions to those produced by the sech-based approximation [6,7]

$$k^{\mathrm{sech}}(1,0,0)=B^{1/2}\left(\frac{1+B}{2}\right)^{3/2}\frac{E^2}{2\sqrt{15}}, \tag{8a}$$

$$k^{\mathrm{sech}}(0,1,1)=\left(\frac{1+B}{2}\right)^{2}\frac{E^2}{2\pi}, \tag{8b}$$

$$k^{\mathrm{sech}}(0,1,-1)=\sqrt{1+\frac{(4\pi^2/15)B}{1+B}}\left(\frac{1+B}{2}\right)^{2}\frac{E^2}{2\pi} \tag{8c}$$

[the out-of-phase sech-based eigenmode (8c) was not derived in Ref. [6], but it can be obtained within the same formalism]. In particular, at the physically important value $B=\frac{2}{3}$, the sets of the eigenfrequencies (7) and (8) are, respectively,

$$\mathbf{k}^{\mathrm{Gauss}}=(0.6211,0.6943,1.0298)\frac{E^2}{2\pi}, \tag{9a}$$

$$\mathbf{k}^{\mathrm{sech}}=(0.5038,0.6943,0.9953)\frac{E^2}{2\pi}, \tag{9b}$$

where the components of the *vector* $\mathbf{k}$ are, in order, the spatial frequencies of the eigenmodes (1,0,0), (0,1,1), and (0,1,-1). At polarization angles other than 45°, however, the eigenmodes cannot be consistently accommodated by the sech-based approximation with equal widths, since at $\theta\neq 45°$, the fixed-point solution has unequal widths ($B=1$ excepted), i.e., equal widths are a nonequilibrium state.

E. Eigenfrequencies and spectral gap

The stability and instability of the different oscillation modes of the perturbed vector soliton can be explained by considering the unperturbed one as a nonlinear structure that protects itself from decay into radiation by placing its eigenfrequency into a spectral gap in which propagating radiation modes do not exist. Generally speaking, this corresponds to the definition of a *gap soliton* [15]. The stationary soliton creates gaps in the linear spectra of oscillatory modes localized around it. For the 45° polarization, the gaps in the spectra of both u and v components are identical, being centered at the mean frequency of the soliton $b_u=b_v\equiv b^{(0)}$. They can be easily found in an exact form from Eqs. (1) linearized around the stationary soliton (no variational approximation is used here):

$$|k-b^{(0)}|<\frac{(1+B)^2}{16/\pi}\frac{E^2}{2\pi}. \tag{10a}$$

For the case of the linear ellipticity, $B=\frac{2}{3}$, the gap (10a) is

$$|k-b^{(0)}|<0.5454\,\frac{E^2}{2\pi}. \tag{10b}$$

The Galilean invariance of the NLS equations (1) implies that the central frequency $b^{(0)}$ can be set equal to zero without loss of generality, so we do this henceforth. For polarization angles other than 45°, the gap widths are different in the u and v subsystems, being determined by the two different propagation constants of the corresponding stationary soliton, that can be found either numerically [16] or by the VA method [8].

If a mode's (spatial) frequency lies inside the continuum (radiation) spectrum (outside the band gap), the oscillation mode couples to the radiation and is therefore subject to decay. If the oscillation mode's frequency is located inside the band gap (outside the continuum spectrum), the oscillations do not couple to the radiation, and they should therefore persist. Harmonics of the small vibrations, generated by the nonlinearity, do give rise to multiple frequencies that resonate with the continuum, but radiative losses through the higher harmonics are usually extremely weak [17].

Compare eigenfrequencies (9) with the spectral gap (10b). The predicted frequency of the relative-position oscillations $k^{\mathrm{sech}}(1,0,0)$ belongs to the gap, while the predicted frequencies of the width oscillations $k^{\mathrm{sech}}(0,1,1)$ and $k^{\mathrm{sech}}(0,1,-1)$ do not. Of the two predicted frequencies of the width oscillations, the frequency of the in-phase mode $k^{\mathrm{sech}}(0,1,1)$ is closer to the gap, and the out-of-phase frequency $k^{\mathrm{sech}}(0,1,-1)$ is farther from it (we begin the analysis with $\mathbf{k}^{\mathrm{sech}}$ rather than $\mathbf{k}^{\mathrm{Gauss}}$ because the numerical results in Sec. III demonstrate that, at $\theta=45°$, the former are closer to the vector soliton's actual spatial frequencies than are the latter.) This suggests that the oscillation of the separation between the centers of the vector soliton's two components should be the stablest eigenmode, while the out-of-phase width oscillations, whose positions are deepest inside the radiation spectrum, should be most unstable. The numerical results presented in Sec. III completely corroborate these predictions.

At *arbitrary* positive values of the cross-coupling coefficient $B\neq\frac{2}{3}$, the in-phase frequency (8b), and out-of-phase frequency (8c) are always outside the gap (10a), while the position-oscillation frequency (8a) is inside the gap when $B<15/17\approx 0.882$. Note that for circular ellipticity ($B=2$) [1] all the three oscillation frequencies (8) are well into the radiation spectrum. The position of the VA-generated eigenvalues relative to the gaps can also be calculated for polarizations other than 45°, but this is physically less important, and the analysis would necessarily be lengthy and technically involved, so we do not pursue it here.

III. TESTING THE MODIFIED GAUSSIAN APPROXIMATION BY PDE SIMULATIONS

We simulated the coupled NLS equations (1) with the cross-phase modulation coefficient $B=\frac{2}{3}$ (corresponding to the linear ellipticity) for a variety of initial conditions. The numerical scheme was the split-step Fourier-transform method with periodic boundary conditions. The pulse widths were measured as the standard FWHM, normalized to match the initial conditions: for initially Gaussian pulses, the widths were computed as the FWHM divided by $2\sqrt{\ln 2}$, and for initially sech-shaped pulses, the widths were computed as the FWHM divided by $2\cosh^{-1}\sqrt{2}$; the two normalizations differ by about 6%.

A. Fixed points

Starting from the usual Gaussian VA's fixed point [Eqs. (2), (3), and (5), or Table I], and numerically propagating the

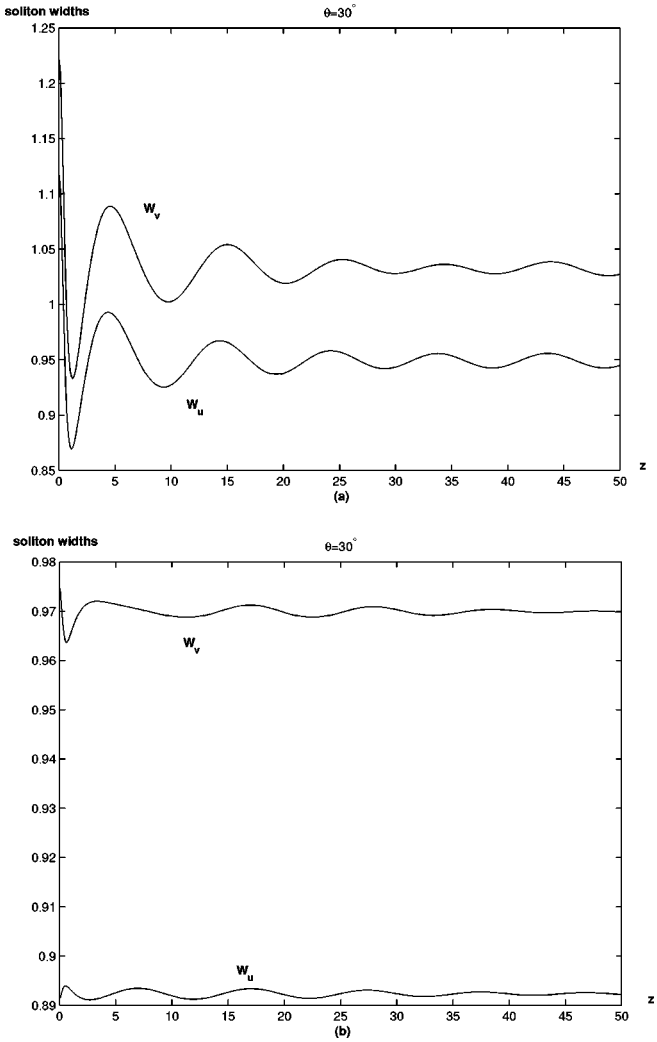

FIG. 1. (a) Evolution of the vector soliton's widths in the PDE's (1) starting from the fixed point predicted by the usual Gaussian approximation [Eqs. (2)–(5)] for the case $\theta=30°$, $E=\sqrt{2\pi}$. (b) Evolution of the widths starting from the corresponding fixed point of the hybrid Gaussian-sech approximation [Eqs. (3)–(6)]. The larger and smaller widths are the less energetic and more energetic components, respectively.

pulse, we observed that slightly more than 99% of the initial energy is ultimately retained by the soliton, with about 1% of the energy lost to emitted radiation. The exact size of the radiative losses depends slightly on the polarization angle θ of the soliton. By this measure—the share of the net energy going into the soliton—the predictions of the usual Gaussian VA are quite good, although the radiative losses ignored by this traditional version of VA are tangible.

If we compare the eventual *widths* of the vector solitons to their initial values, the traditional Gaussian-based VA gives a not-so-good agreement with the numerical results. The FWHM widths at the end are about one-sixth smaller than at the start. This is, as expected, due to the inherent inaccuracy of the Gaussian *Ansatz* (see Sec. II C), but it is a serious drawback nonetheless. To illustrate, Fig. 1(a) shows the numerically simulated evolution of the pulse widths, starting from the fixed point of the usual Gaussian approximation, with the total energy $E=\sqrt{2\pi}$ and polarization $\theta=30°$.

The hybrid Gaussian-sech approximation, proposed Sec. II and based on Eqs. (3)–(6), proves to give much more accurate predictions for the stationary states than the usual Gaussian VA. The less energetic component's width (the larger of the two) predicted by the hybrid approximation is slightly farther from the numerical results than the (smaller) width of the more energetic component. There is some dependence on the vector soliton's polarization angle—the larger the asymmetry between the components, the larger the error—but even in the worst case the prediction exceeds the eventual result by only $\lesssim 1\%$ (and in this worst case for the less energetic component, the predicted width of the more energetic one is found to be extremely accurate). Comparing this with the above-mentioned error of the traditional Gaussian VA, that predicted widths are greater than the actual values by about one-sixth, we conclude that the empirically modified approach improves the VA accuracy, defined in terms of the static widths, by a factor of more than 15; and, as explained above, the modified model [Eqs. (3)–(6)] identically coincides with the exact result in the integrable cases $\theta=0°$, 45°, and 90°. The radiative energy shed by the evolving vector soliton was too small to measure, in contrast with the case of the usual Gaussian approximation, with quite appreciable radiative energy losses $\approx 1\%$, which is another drastic improvement offered by the hybrid VA model.

For example, for the vector soliton with polarization $\theta=15°$, the hybrid model gives the width of the more energetic component, against the numerically computed value, to within an error of $\pm 0.05\%$, and the width of the less-energetic component is 1.1% more than the numerically computed final width. At $\theta=30°$, the hybrid model gives the less energetic component's width as 0.5% too high, and the more energetic component's width as 0.1% too low. Figure 1(b) illustrates this, showing the evolution of the widths in the PDE simulations, starting from the fixed point of the hybrid model with the total energy $E=\sqrt{2\pi}$ and polarization $\theta=30°$. In the limiting case when nearly all the energy is in one component, the equation for the other component can be linearized and an exact solution for it can be obtained (see, for example, Ref. [18]); in this case, the modified VA based on Eqs. (3)–(6) overestimates the FWHM of the quasilinear component by just under 1.5%.

B. Oscillations

Near equilibrium, the Gaussian VA [Eqs. (2)–(4)] predicts three small-vibrational modes, as described in Sec. II D. In the PDE simulations, the most persistent mode was found to be oscillations of the separation between the two components of the soliton. The next most persistent mode were in-phase oscillations of the two widths. The out-of-phase width vibrations were found to be more than merely less persistent than the other two modes; this mode proved to be unstable, showing a clear tendency to rearrange itself into the in-phase vibrational mode (we stress that this is not a radiative instability): the initially out-of-phase vibrations of the two widths eventually synchronize themselves into the in-phase vibrations, but without shedding more radiation than comparable in-phase vibrations (very little radiation is emitted in either case). This numerical observation is in an apparent contrast with the predictions of the VA model,

which provides no mechanism to account for this effect. However—bringing in another analytical tool to complement the VA—consideration of the spectral gap offers an explanation. Although the rearrangement of the out-of-phase oscillation mode into the in-phase one is not accompanied by a conspicuous emission of radiation in the numerical simulations, the former mode's instability is directly predicted by the analysis presented in Sec. II: this mode is expected to be strongly unstable because it is located far *outside* the stability-providing band gap. The gap, actually, should be compared to the numerically computed eigenfrequencies of the three modes, rather than to the frequencies predicted by the VA; this will be done in detail below for the 45° polarization. As for the fact that practically no radiation is finally emitted in the course of the rearrangement of the unstable mode into the stable one, this may be explained as follows: the radiation released by the decaying unstable mode is immediately captured by the growing stable one, helping to build up the in-phase width oscillations. In principle, the energy exchange between the vibrational modes can be incorporated into the extended VA by adding extra degrees of freedom to the *Ansatz*, as was done by Kath and Smyth for the single NLS equation [11]; however, for the coupled NLS equations, such an investigation turns out to be extremely involved, and is therefore not included in this work.

Comparing the VA predictions with the PDE simulations shows that the oscillation frequencies and eigenvectors are fairly well predicted by VA when the energy is nearly evenly divided between the components. When the energy is almost entirely concentrated in one component, the predictions are also quite accurate, but for a trivial reason—the importance of the less-well-predicted, less-energetic component decreases as its energy decreases.

We start with polarization $\theta=45°$. For the mode in which the predictions based on the usual Gaussian and sech approximations disagree the most, small oscillations of the separation between the centers of the two vector soliton components [see Eqs. (9)], the PDE results are (quite naturally) closer to the sech model's predictions: the simulations yield the frequency $k^{\mathrm{num}}(1,0,0)=0.53(E^2/2\pi)$, compared to $k^{\mathrm{sech}}(1,0,0)=0.50(E^2/2\pi)$ and $k^{\mathrm{Gauss}}(1,0,0)=0.62(E^2/2\pi)$ for the usual sech-based and Gaussian approximations. The in-phase width oscillations prove to be slower than predicted: $k^{\mathrm{num}}(0,1,1)=0.54(E^2/2\pi)$ in the PDE simulations, compared to $k^{\mathrm{sech}}(0,1,1)=k^{\mathrm{Gauss}}(0,1,1)=0.69(E^2/2\pi)$ produced by both variational approximations (7b) and (8b). In contrast to these results, the out-of-phase width oscillations turn out to be very significantly slower than predicted by the VA (although the measurements in the simulations is difficult due to the instability of the mode): the numerically computed frequency is $k^{\mathrm{num}}(0,1,-1)=0.56(E^2/2\pi)$, compared to $k^{\mathrm{sech}}(0,1,-1)=0.99(E^2/2\pi)$ [Eq. (7c)] or $k^{\mathrm{Gauss}}(0,1,-1)=1.03(E^2/2\pi)$ [Eq. (8c)].

Equation (10) yields, for $\theta=45°$, a spectral gap of width $0.5454(E^2/2\pi)$. Thus the above-mentioned numerically computed frequency $k^{\mathrm{num}}(1,0,0)=0.53(E^2/2\pi)$ of the position-oscillation eigenmode is indeed *inside* the gap, while the in-phase width-oscillation eigenmode's frequency $k^{\mathrm{num}}(0,1,1)=0.54(E^2/2\pi)$ is almost exactly at the gap's edge, and the out-of-phase width-oscillation eigenmode's frequency $k^{\mathrm{num}}(0,1,-1)=0.56(E^2/2\pi)$ is definitely *outside* the gap.

The in-phase vibrational mode looks, numerically, like an attractive dynamical regime. Starting from initial conditions corresponding to a mixture of the in-phase and out-of-phase modes, we always observed the out-of-phase component to die out much faster than the in-phase mode. The numerical simulations showed that the drop of the out-of-phase mode's amplitude is *not* a result of radiative losses—very little radiation is emitted by the vibrating vector soliton in the course of its evolution. A more detailed analysis of the numerical results offers another explanation for the effect, based on consideration of the model's Hamiltonian. The soliton vibrations are a part of the total Hamiltonian H (the static soliton is at a minimum H). For the same amplitude, the Hamiltonian of the out-of-phase vibrational mode is found to be about twice as large as the Hamiltonian of the in-phase vibrational mode. So at a given value of H the oscillations transforming from out of phase to in phase should decrease in amplitude.

The VA predictions, compared to the PDE-simulation results, grow worse when one component has more energy than the other. The computed frequencies then tend to be smaller than the analytic predictions. At the polarization $\theta=30°$, the PDE simulations give a frequency of the relative-position oscillations $k^{\mathrm{num}}(1,0,0)=0.49(E^2/2\pi)$, compared to $k^{\mathrm{Gauss}}(1,0,0)=0.65(E^2/2\pi)$ in the Gaussian-based approximation (the usual sech-based approximation does not apply to polarizations different from 45°). The frequency of the in-phase width oscillations was found numerically to be $k^{\mathrm{num}}(0,1,1)=0.65(E^2/2\pi)$, compared to $k^{\mathrm{Gauss}}(0,1,1)=0.76(E^2/2\pi)$ in the Gaussian model. The out-of-phase oscillation mode was found to be very unstable at the polarizations different from 45°, so that its frequency could not be computed accurately. To make another comparison: at the same polarization, $\theta=30°$, but without coupling between the components, $B=0$, the standard variational prediction is $k^{\mathrm{sech}}=0.56(E^2/2\pi)$ for the width oscillations in the more energetic component.

At the polarization $\theta=15°$, the PDE simulations give the frequency of the relative-position oscillations $k^{\mathrm{num}}(1,0,0)=0.46(E^2/2\pi)$, compared to $k^{\mathrm{Gauss}}(1,0,0)=0.69(E^2/2\pi)$. The in-phase frequency was found to be $k^{\mathrm{num}}(0,1,1)=0.74(E^2/2\pi)$, compared to $k^{\mathrm{Gauss}}(0,1,1)=0.90(E^2/2\pi)$. The out-of-phase oscillation mode was again too unstable for its frequency to be computed. Without coupling ($B=0$), the variational prediction would be $k^{\mathrm{sech}}=0.87(E^2/2\pi)$ for the width oscillations in the more energetic component.

In addition to this, the simulations reveal that, in the course of each oscillation cycle, the less energetic component peaks slightly later than the more energetic one, and the less energetic component does not oscillate by as much (relative to the more energetic component) as predicted by the VA (see Table II). As predicted, at $\theta=45°$, the widths W_u and W_v vary by the same amount during oscillation. Not as predicted, at $\theta=30°$ and at $\theta=15°$, the widths of the two components also oscillate by the same amount during the oscillations; the VA predicts the less energetic component's width varying by more than the width of the more energetic component. The width of the less energetic component may peak (or bottom out) after the more energetic component, the

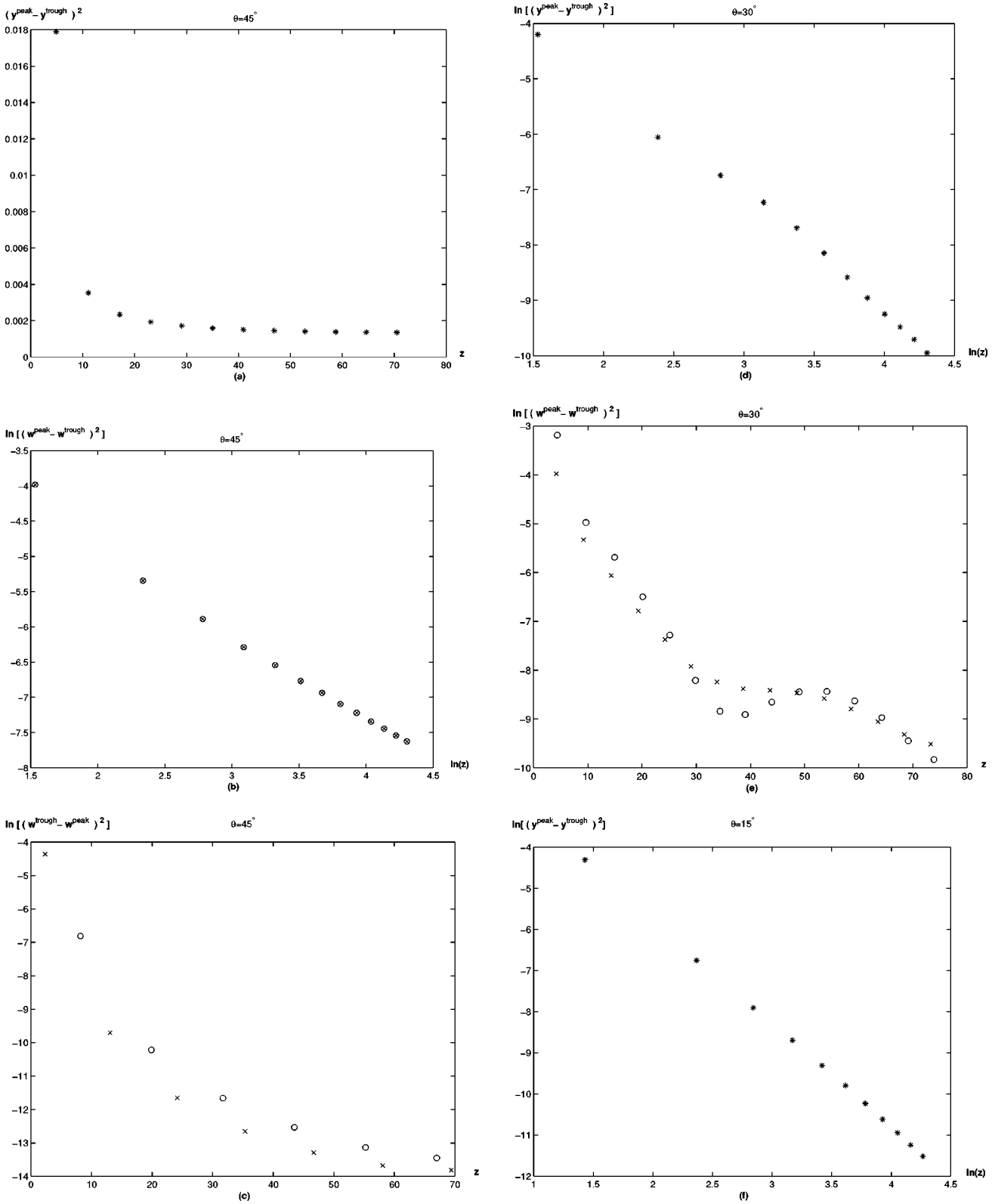

FIG. 2. Typical examples of evolution of the vibrational modes in direct numerical simulations of the coupled NLS equations (1) with the cross-phase modulation coefficient $B=\frac{2}{3}$. Parts (a)–(c) have polarization $\theta=45°$, parts (d) and (e) have $\theta=30°$, and parts (f) and (g) have $\theta=15°$. All the simulations were performed for the energy $E=\sqrt{2\pi}$. The asterisk indicates the separation y between the components [parts (a), (d), and (f)]; a cross (x) is the width of the u component, and a circle *(o)* is the width of the v component [parts (b), (c), (e), and (f)]. The vertical axes show the peaks (or troughs) of the soliton parameters minus the previous troughs (or peaks), squared; part (c) is an exception, showing the troughs only (to better illustrate a switch from the out-of-phase to in-phase oscillations). The horizontal axes show the positions z at the forward of the peaks or troughs. The initial pulses are sech shaped, with the vector soliton's initial parameters taken at the fixed point predicted by the hybrid VA, except for the initial separations in the panels (a), (d), and (f), which are added as perturbations to the predicted fixed points in order to excite the separation oscillations.

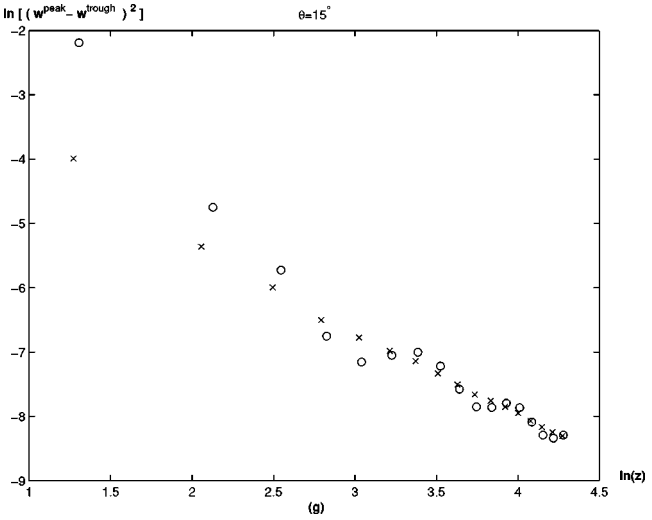

FIG. 2. (*Continued*).

delay generally being from 5% to 10% of the oscillation period. A general conclusion suggested by the simulations of the full PDEs (1) is that the two components of the vector soliton oscillate more or less separately when the energy is distributed unevenly between them, with the more energetic one dominating and the less energetic one being pulled along. This feature can be conceived in the following way: the more energetic component has, by itself, a higher frequency of the internal width vibrations than the less energetic one, so it will tend to oscillate faster, running ahead of the less energetic component. The relatively small oscillations (compared to the VA prediction) of the less energetic component (the less energy in the component, the greater the disparity between the VA prediction and the numerical results) are consistent with this component's being merely driven (pulled along) by the more energetic one when the energy is split unevenly. The more uneven the division of energy, the more the oscillating vector soliton will resemble a composite of two relatively weakly coupled, separate single-component solitons, rather than a single unit. This trend is compatible with the above-mentioned circumstance that, in the limiting case when the energy of the subordinate component is much smaller than in the leading one, the intrinsic nonlinearity of the weak component may be neglected, so that it becomes a linear mode governed by the leading component [18].

Figure 2 illustrates the dynamics of various oscillation modes. The vertical axes measure the changing Hamiltonians of the oscillation modes. For the small oscillations near equilibrium, the Hamiltonians of the oscillation modes are proportional to the squares of the maximum variations from equilibrium. The VA models yield constants of proportionality, but different ones for the different *Ansätze* (sech, Gaussian, or hybrid); and inferring the constants of proportionality from the direct numerical PDE simulations gives yet different values. Provided the perturbations are small, the peaks (or troughs) of the soliton parameters minus the previous troughs (or peaks), squared, gives the Hamiltonian up to a multiplicative constant. The symbols used are: asterisks (*) for the separation (y), and crosses (x) and circles (o) for the widths of the u and v components, respectively. The positions z on the horizontal axes are the locations of the forward peaks or troughs. Figure 2(a) shows the separation mode of a $\theta=45°$ soliton, on a straight scale. A remarkable feature displayed by this plot is *saturation*: the decay virtually ceases at a finite amplitude. Figure 2(b) is a log-log plot of the in-phase width oscillations of a $\theta=45°$ soliton. The approximately straight line yields a power-law decay $\sim z^{-1.07}$. Note that the power-law decay is very slow in comparison with other common forms of loss, such as the exponential decay which would be caused by dissipative losses. Figure 2(c) shows the evolution of an initially out-of-phase–perturbed $\theta=45°$ soliton (initial widths are $[(6/5)\sqrt{2/\pi}\pm 0.1)]$, with a log scale on the vertical axis. There is only one data point per period—only the troughs are displayed here—unlike the other plots which show both peaks and troughs. While initially the troughs of the two components are exactly out of phase, after six periods the two components are more than halfway to being in-phase. Note that the oscillations of the component which is catching up are larger than those of the advanced component.

Figure 2(d) shows the separation mode of a $\theta=30°$ soliton, starting with the equilibrium widths predicted by the hybrid VA. This mode is less stable than in the case of $\theta=45°$ polarization: after some settling down of the widths, the vibrational Hamiltonian decays according to a power law $\sim z^{-2.4}$ (note no saturation). Figure 2(e) shows nearly in-phase width oscillations of the $\theta=30°$ soliton. The waviness of the oscillation modes' slopes (oscillations of the widths of components u and v represented by crosses and circles, respectively) is due to the disappearing out-of-phase component. The decay is very roughly $\sim z^{-2.}$, although the presence of the dying out-of-phase component obscures this. Also note that the extrema of the less energetic component v (circles) are slightly delayed compared to those of the more energetic component u (crosses).

Lastly, Fig. 2(f) shows a log-log plot of the separation mode of the $\theta=15°$ soliton. The corresponding widths (which are not displayed) are initially at the fixed point produced by the hybrid VA, and suffer only a very slight readjustment in the course of the simulations. The decay is a power law, roughly $\sim z^{-2.7}$. Figure 2(g) is a log-log plot of the nearly in-phase width oscillations of the $\theta=15°$ soliton. The intersections in the plot are, as well as in Fig. 2(e), from the quickly disappearing out-of-phase component. The decay rate is very roughly $\sim z^{-1.3}$, although the dying out-of-phase component obscures this. Observe that the vibrational phase of the less energetic component v (circles) is delayed compared to the more energetic one u (crosses).

For the $\theta=45°$ soliton, the leveling off (saturation) of the relative-position oscillation at a nonzero amplitude [Fig. 2(a)], the decay of the in-phase width oscillations at a rate slightly faster than z^{-1} [Fig. 2(b)], and the quick decay of the out-of-phase oscillations [Fig. 2(c)] generally comply with the numerical observations reported in the very recent work [3]. However, that work addresses details of the oscillations only in certain limits, yielding less information about gradually decaying vibrations than about persistent ones. The instability of the out-of-phase vibrations with respect to the in-phase vibrations [Figs. 2(c), 2(e), and 2(g)] is not captured in Ref. [3], nor is the fact that the less energetic component tends to be delayed in relation to the more energetic one [Figs. 2(e) and 2(g)]. At polarizations $\theta\neq 45°$, Ref. [3] pre-

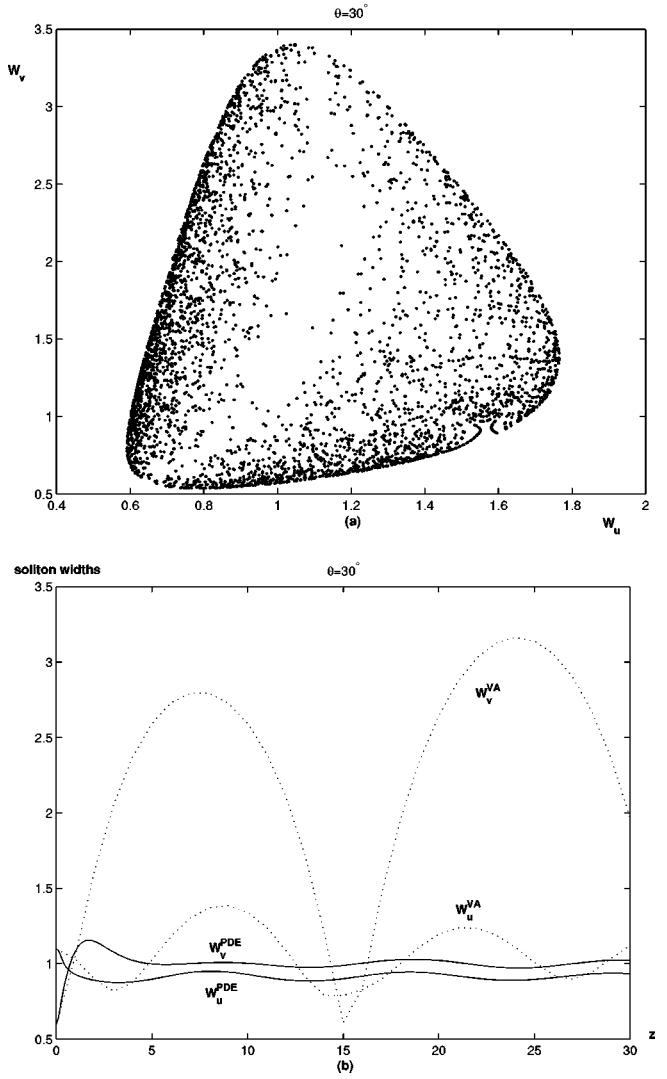

FIG. 3. (a) The Poincaré map generated by a typical dynamical trajectory of the ODE approximation [Eqs. (3)–(6)] with $\theta=30°$ and $E=\sqrt{2\pi}$, starting from initial conditions $W_u^{\rm sech}=1.1$ and $W_v^{\rm sech}=0.6$, the initial separation y and phases being zero. (b) Evolution of the widths of the two vector soliton's components vs the propagation distance z, starting from the same initial conditions as (a); the solid lines are the PDE results, and the dotted lines are obtained from the ODEs (4) derived by means of the variational approximation.

dicts permanence of the position oscillation mode, whereas our numerical simulations showed no such permanence [see Figs. 2(d) and 2(f), for example].

C. Absence of true dynamical chaos

The VA approximation predicts a possibility of dynamical chaos in the vector soliton's internal vibrations with a sufficiently large amplitude, most noticeably in the case combining the in-phase and out-of-phase width oscillations. For example, Fig. 3(a) shows the Poincaré map produced by a single dynamical trajectory generated by the ODEs (4). This Poincaré map is clearly space filling, corresponding to a chaotic motion. But in the corresponding PDE simulations, the out-of-phase component dies out too quickly for chaos to appear. Figure 3(b) shows the chaotic trajectory from Fig. 3(a) side by side with the evolution of the same dynamical variables (the two widths) in the PDE simulations, starting from the identical initial conditions. This illustrates a fairly generic conclusion supported by a number of runs: in the cases where the ODEs produced by the variational approximation predict dynamical chaos, the PDE simulations demonstrate that, in reality, the large-amplitude oscillations *always* decay (and for the out-of-phase mode, even small-amplitude oscillations decay) so quickly that the vector soliton internal vibrations do not exhibit dynamical chaos.

IV. CONCLUSIONS

The variational approximation's predictions for the dynamics of a two-component vector soliton governed by a pair of coupled NLS equations were examined in detail. Looking at the system as a nonlinear structure protected from decay by the spectral gaps, and comparing the vector soliton's vibrational frequencies with the spectral gaps, yields additional predictions concerning stability of the different vibrational modes. The predictions were systematically tested against direct numerical simulations of the PDEs. Generally, agreement was good, consistent with previous works, which demonstrated that the variational approximation usually yields very reasonable results [6–11]. Starting from the initial conditions corresponding to the fixed points predicted by the Gaussian *Ansatz*, PDE simulations showed that (for the case of the linear ellipticity) over 99% of the initial energy goes into the final pulse, and the rest (still an appreciable share) is lost to radiation. However, the vector soliton's widths decrease by about a sixth. Because of these errors, the traditional variational approximation based on the Gaussian *Ansatz* is in some respects not very (or at all) close to the genuine stationary states, and so is sometimes a poor tool to analyze the vector soliton's small-vibrational modes or other subtle effects; this approximation nevertheless yields three fundamental eigenmodes qualitatively correctly and to a degree quantitatively correctly.

To remedy these drawbacks of the Gaussian approximation, we have proposed a hybrid variational technique, using both the Gaussian—to produce the finite-dimensional dynamical system, which is the essence of the variational approximation—and a sech *Ansatz*—to readjust the vector soliton's shape at the end. This hybrid model gives an excellent approximation for the stationary states, so that the radiative losses are virtually absent, and the widths are predicted to no worse than within about 1% of the numerically found values. While the averaged Lagrangian method using sech from the start [6,7,10] is fully tractable only if the two widths are postulated to be identically equal, and the variational method using the Gaussian pulses from the start is fully tractable but less accurate, the hybrid approximation maintains the tractability and flexibility of the Gaussian approximation and the accuracy of the sech approximation. Given that the variational models (except for the sophisticated modification put forward in Ref. [11]) do not include the radiation modes, the fact that the steady states predicted by the hybrid approach, on comparison with numerical simulation of the PDE's, suffer virtually no radiation loss is a significant advantage.

When the vector soliton's energy is nearly evenly divided

between the polarization components, two of the small-vibrational modes predicted by the hybrid variational approximation—vibration of the separation between the centers of the two components, and the in-phase oscillations of the two widths—agree well with the direct simulations. The vibrations of the separation turn out to be most persistent, and the in-phase width vibrations are also fairly long lasting. The third eigenmode, the out-of-phase vibrations of the two widths, is, in contrast to the variational models' predictions, unstable against conversion into the in-phase width vibrations: initially out-of-phase vibrations tend to quickly synchronize themselves, becoming in-phase after a few periods.

Both the stability of the first two eigenmodes and the instability of the third eigenmode can be easily explained by comparing their frequencies to the soliton-induced gaps in the radiation spectra: The first and second frequencies are inside and at the edge of the spectral gap, making the modes, respectively, very stable and marginally stable. The third frequency is located well into the continuum (radiation), allowing energy to couple out of it, thus strongly destabilizing the eigenmode.

In the case when the energy is divided nearly equally between the two components, the analysis has revealed a noteworthy feature quite important for the physical applications (first of all, to the solitons in nonlinear optical fibers): the gradual decay of the separation mode ceases at a final level of its amplitude (*saturation*), so that this mode appears to be absolutely robust, persisting indefinitely long. Unlike this, the relatively stable in-phase width oscillation mode decays according to a power law (which is much slower than exponential decay).

When the energy is unevenly divided between the components, the variational predictions for the stationary states grow worse for the less energetic component, but better for the more energetic one. Out of equilibrium, the component with less energy tends to be driven by vibrations of the dominant component, rather than contributing to the oscillations in an equal manner, as the averaged Lagrangian variational approximation has it. In the case of uneven energy distribution, the separation mode loses its remarkable robustness, and becomes subject to a slow power-law decay.

Finally, we considered the possibility of chaotic internal oscillations of the vector soliton. Dynamical chaos is clearly exhibited by the sixth-order ODE system generated by the variational approximation. In the PDE simulations, however, chaos is never observed. This can be explained by the fact that the quickly decaying out-of-phase width-oscillation mode leads to degeneration of the large-amplitude internal vibrations.

ACKNOWLEDGMENTS

We appreciate stimulating discussions with Y. Silberberg and Y. Barad.

[1] G. P. Agrawal, *Nonlinear Fiber Optics* (Academic, San Diego, 1995).
[2] S. V. Manakov, Zh. Eksp. Teor. Fiz. **65**, 505 (1973) [Sov. Phys. JETP **38**, 248 (1974)].
[3] J. Yang, Stud. Appl. Math. **98**, 61 (1997).
[4] D. Anderson, Phys. Rev. A **27**, 3135 (1983).
[5] V. E. Zakharov and A. B. Shabat, Zh. Eksp. Teor. Fiz. **61**, 118 (1972) [Sov. Phys. JETP **34**, 62 (1972)].
[6] T. Ueda and W. L. Kath, Phys. Rev. A **42**, 563 (1990).
[7] B. A. Malomed, Phys. Rev. A **43**, 410 (1991).
[8] D. J. Kaup, B. A. Malomed, and R. S. Tasgal, Phys. Rev. E **48**, 3049 (1993).
[9] D. Anderson, M. Lisak, and T. Reichel, J. Opt. Soc. Am. B **5**, 207 (1988).
[10] D. J. Muraki and W. L. Kath, Phys. Lett. A **139**, 379 (1989); Physica D **48**, 53 (1991).
[11] W. L. Kath and N. F. Smyth, Phys. Rev. E **51**, 1484 (1995).
[12] C. Etrich, U. Peschel, F. Lederer, B. A. Malomed, and Y. S. Kivshar, Phys. Rev. E **54**, 4321 (1996).
[13] D. Anderson, M. Lisak, B. Malomed, M. Quiroga-Teixeiro, and L. Stenflo, Phys. Rev. E **55**, 1677 (1997).
[14] Y. Barad and Y. Silberberg, Phys. Rev. Lett. **78**, 3290 (1997).
[15] C. M. de Sterke and J. E. Sipe, Prog. Opt. **33**, 203 (1994).
[16] M. Haelterman, A. P. Sheppard, and A. W. Snyder, Opt. Commun. **103**, 145 (1993).
[17] B. A. Malomed, Physica D **27**, 113 (1987).
[18] B. A. Malomed, J. Opt. Soc. Am. B **9**, 2075 (1992).
[19] B. A. Malomed, P. D. Drummond, H. He, D. Anderson, A. Berntson, and M. Lisak, Phys. Rev. E **56**, 4725 (1997).